

# MuPix: an HV–MAPS for the Mu3e experiment

Heiko AUGUSTIN<sup>1</sup>, Niklaus BERGER<sup>3</sup>, Sebastian DITTMEIER<sup>1</sup>, Florian FRAUEN<sup>1</sup>, David Maximilian IMMIG<sup>1</sup>, Dohun KIM, Richard LEYS<sup>2</sup>, Lukas MANDOK<sup>1</sup>, Annie MENESES GONZALEZ<sup>1</sup>, Marius MENZEL<sup>1</sup>, Ivan PERIĆ<sup>2</sup>, André SCHÖNING<sup>1</sup>, Jakob STRICKER<sup>1</sup>, Luigi VIGANI<sup>1</sup>, Alena WEBER<sup>1,4</sup> and Benjamin WEINLÄDER<sup>1</sup>

<sup>1</sup>Physikalisches Institut, Universität Heidelberg, Im Neuenheimer Feld 226, 69120 Heidelberg, Germany

<sup>2</sup>Institut für Prozessdatenverarbeitung und Elektronik, KIT, Hermann-von-Helmholtz-Platz 1, 76344 Eggenstein-Leopoldshafen, Germany

<sup>3</sup>Institut für Kernphysik, Johannes Gutenberg-Universität Mainz, Johann-Joachim-Becherweg 45, 55128 Mainz, Germany <sup>4</sup>Now Robert Bosch GmbH, Reutlingen, Germany

E-mail: [vigani@physi.uni-heidelberg.de](mailto:vigani@physi.uni-heidelberg.de)

(Received January 20, 2023)

Mu3e is an experiment based at PSI which searches for the charged lepton flavour violating decay  $\mu^+ \rightarrow e^+e^-e^+$  with an aimed sensitivity of 1 event in  $10^{16}$  decays. The low energy of the decay products imposes harsh constraints to the momentum resolution and, ultimately, to the material budget. Among the several measures to minimize the material budget, the vertex detector adopts the HV-CMOS technology. Thanks to this, the chips can be thinned to  $50\mu\text{m}$  while keeping high efficiency and time resolution. In addition, the powering and data transmission is performed by means of kapton-aluminum High Density Interconnects, which serve as mechanical support as well. Starting from the detector concept, this talk will outline the challenges faced by the pixel detector chip, the MuPix, and the solutions adopted. Finally, the latest results from the R&D phase and the first detector prototypes will be shown.

**KEYWORDS:** hvcmos, pixel, tracker, hvmaps

## 1. Introduction

The MuPix chips are a series of sensors designed for the Mu3e experiment [1]. The goal of the experiment is to investigate the  $\mu^+ \rightarrow e^+e^-e^+$  decay channel, achieving a final single event sensitivity of  $10^{-16}$ . This is planned to be reached in two phases. During Phase 1, the experiment will be located in the  $\pi e5$  beamline of the Paul Scherrer Institut (PSI), Switzerland. This beamline can deliver muons up to fluences of the order of 100 MHz. Next, for Phase 2, the planned High-Intensity Muon Beamline will be used, which will deliver muons at a fluence of 1 GHz. As the muons decay at rest, the electrons and positrons originating from the muon decays have an energy of at maximum 53 MeV/c. These features lead to very tight experimental requirements, especially in terms of material budget as well as spatial and time resolution. The MuPix is therefore designed to fulfil these requirements, as the final goal is to detect rare events at high rate and precision. In particular, the constraints on the tracker spatial resolution require a single pixel resolution of at least  $30\mu\text{m}$ . The pixel pitch is designed to be  $80\mu\text{m}$ , which allows for a single pixel spatial resolution of at worst  $80\mu\text{m}/\sqrt{12} \sim 23\mu\text{m}$ , well below the aforementioned requirement. The continuous nature of the muon beam and its high rate enforces the usage of a triggerless readout, with a maximum allowed time resolution of 20 ns. To maintain a low material budget, the total thickness of the sensor, both electronics and silicon bulk, is reduced to  $50\mu\text{m}$ .

The development of the MuPix has been conducted for several years. The design is based on the com-

mercial IBM 180 nm process, produced by AMS until 2018 and by TSI Semiconductors afterwards. As of 2022, several prototypes have been produced, among which MuPix10 and MuPix11. MuPix11, in particular, is foreseen to be used for the construction of the Mu3e tracker.

## 2. Design

### 2.1 Overview

The MuPix design is based on the High-Voltage Monolithic Active Pixel Sensor (HV-MAPS) technology [2]. With this technique the readout electronics are embedded in the silicon bulk inside a deep n-well, which is in contact with the p-substrate. This way a high reverse bias voltage can be applied to the deep n-well without affecting the readout electronics themselves. A large depletion zone is then formed between the deep n-well itself and the p-substrate. Thanks to this feature, charges can be collected from a depth of several tens of micrometers, and the resulting signal is larger and faster than the one collected by conventional MAPS. These characteristics, along with the possibility of thinning the wafers to few tens of micrometers, lead to the choice of this technology for the Mu3e tracking system.

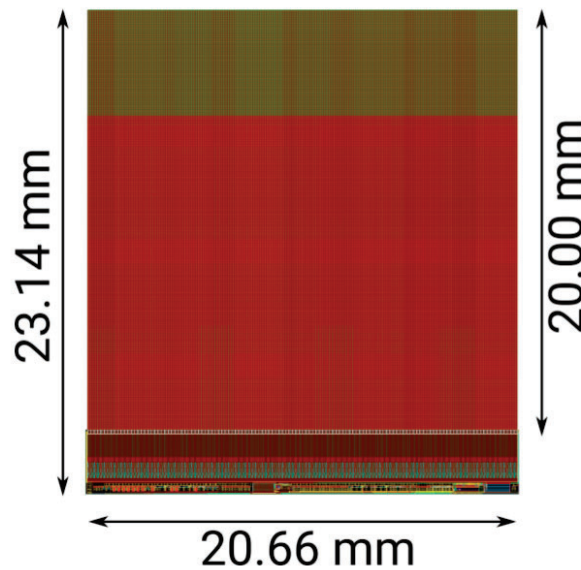


**Fig. 1.:** Layout of MuPix10 from [4]. Figure not in scale.

The results presented in this article are collected with MuPix10 prototypes. At the time this article is written, the first MuPix11 prototypes have been produced and their characterization has just started, therefore no final results could be collected. The MuPix10 [4] is the first full-scale chip, produced to fulfil all the experimental requirements of Mu3e. Its total size is  $20.66 \times 23.14 \text{ mm}^2$ , with an active area of about  $20 \times 20.48 \text{ mm}^2$ . The active area consists of  $256 \times 250$  quadratic pixels each with a  $80 \mu\text{m}$  pitch. A layout of the chip design can be seen in Figure 1.

To further reduce the material budget, the flex boards used to readout the MuPix sensors in Mu3e are foreseen to be produced with Aluminum-Kapton foils and to implement only two layers [5]. Given the limited amount of lines that can be driven through these flex boards, the MuPix sensors are designed to operate with as few connections as possible. For instance, the electronics can be operated with just

two external voltage levels, VDD, which is set to 1.8 V, and ground (GND). Another voltage level is used to operate the amplifiers, which in the case of MuPix10 can be internally generated. The high voltage is supplied externally. To communicate with the chip, two LVDS pairs are foreseen: the clock (125 MHz) and the serial input, both of them operating as bus lines. The data are sent out through up to 4 1.25 Gbit/s LVDS links, namely links A, B, C and D. Each of the first three data links is connected to one specific pixel submatrix (A, B or C), while link D uses the multiplexed output of the others.

Depending on the settings, the total power consumption lays between 200 and 250 mW/cm<sup>2</sup> [4].

## 2.2 Pixel Read-out

The basics of the readout architecture are the same for every MuPix prototype. The electron-hole pairs produced by an incident particle are driven to the collecting diode by the electric field produced by the high reverse bias voltage. The signal is then amplified by an in-pixel Charge Sensitive Amplifier (CSA) and driven by a source follower to the chip periphery. There, every pixel in the active area is mirrored by a digital partner cell, where the output from the CSA is compared against a threshold by a comparator. This produces a digital signal for as long as the CSA output stays over the threshold. The moment when the signal is issued (i.e. when the CSA output crosses the threshold) is known as Time-of-Arrival (ToA). The moment when the signal is released (when the CSA output falls back below threshold) is known as trailing edge. The duration of this signal is called Time-over-Threshold (ToT), and is related to the CSA output amplitude, and ultimately to the total collected charge. In the MuPix architecture, the leading edge and the trailing edge time is sampled with a clock whose frequency is derived from the main clock. Furthermore, the comparator threshold can be adjusted at the single pixel level by means of dedicated DACs, referred to as TDACs. The hit information is stored in the digital cell and read out by a state machine in the periphery, which sends the hit data out via the data lines.

A detailed schematic of the read-out chain is shown in Figure 2.

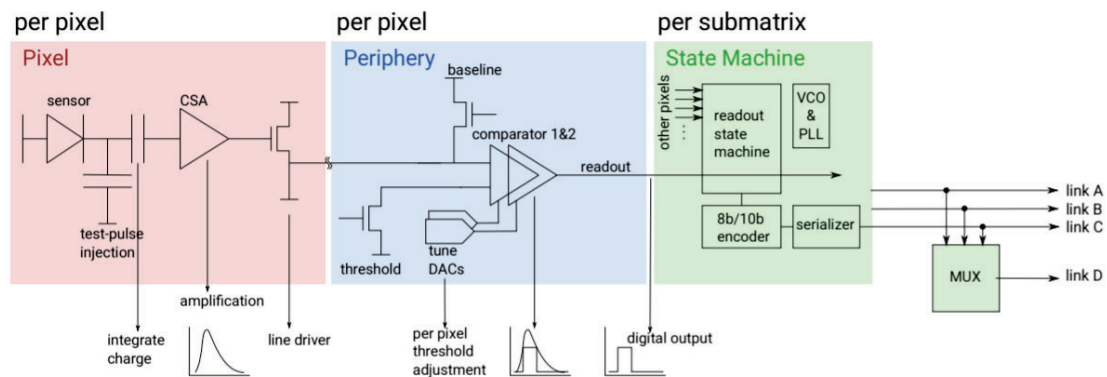


**Fig. 2.:** Schematics of the MuPix read-out. From [4]

## 3. Characterization Results

### 3.1 100 $\mu$ m Thick Chips

The first batch of MuPix10 prototypes to be characterized consists of chips produced on wafers of 370(20)  $\Omega$  cm resistivity. The chips are thinned to 100  $\mu$ m without any back-side processing. This thickness was chosen as a starting point in the characterization of MuPix10 as the dices are easier

to handle than the  $50\text{ }\mu\text{m}$  ones. The breakdown voltage in this case is observed to be about 115 V. A series of lab tests and test beams has been performed to evaluate the performance of these prototypes.

### 3.1.1 Efficiency

The sensor efficiency has been measured with a telescope consisting of MuPix10 sensors itself at the DESY testbeam facility [12], with  $4\text{ GeV}/c^2$  electrons. During this campaign, samples produced from  $370\text{ }\Omega\text{cm}$  resistivity wafers have been studied. A comprehensive scan of the efficiency as a function of the threshold and the bias voltage is shown in Figure 3 for a  $370\text{ }\Omega\text{cm}$  resistivity dice. The data show that the sensor can reach values of efficiency higher than 99% at already 30 V of bias.

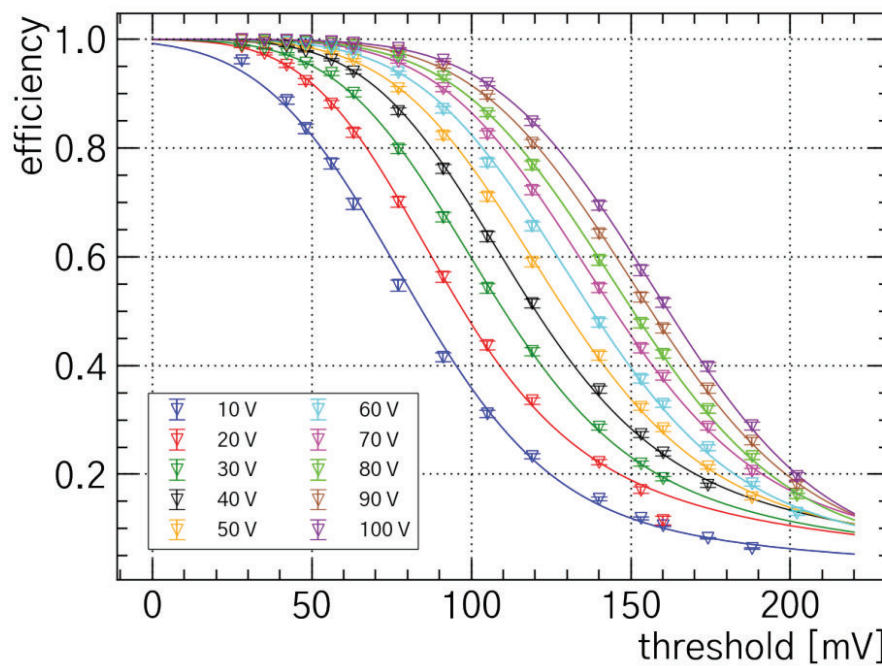


**Fig. 3.:** Efficiency as a function of threshold for a  $100\text{ }\mu\text{m}$  thin MuPix10 sensor at different biases. The data are fitted with the predicted integral function of the Landau-Gauss convolution [8]

### 3.1.2 Threshold Tuning

As described in section 2.2, the comparator threshold can be regulated at the single pixel level via the TDACs, a procedure known as threshold tuning. One of the possible strategies for threshold tuning consists of measuring each pixel's threshold by injecting charge into the CSA, and then setting each pixel's TDAC to obtain the smallest threshold dispersion. This strategy has been verified with MuPix10, and its result is shown in Figure 4. The threshold dispersion is significantly reduced, from a value of  $240\text{ e}$  to a value of  $75\text{ e}$ .

### 3.1.3 Time resolution

The time resolution has been measured in the lab with a  $\text{Sr}^{90}$  source by comparing the Time of Arrival on chip with the time recorded by a reference scintillator, as the chip is placed between the source and the scintillator itself.

There are several factors that affect the time resolution, some of which can be corrected for by correlating with the hit information. In the MuPix architecture two effects can be observed: the line delay

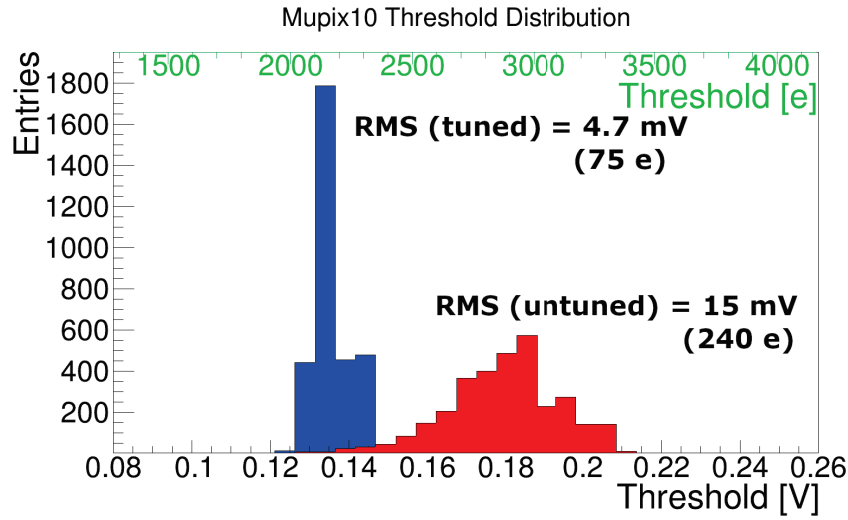


**Fig. 4.:** Threshold distribution obtained with injection for MuPix10 before (red) and after (blue) threshold tuning. From [1].

and the time-walk [3]. The first one is a delay due to the capacitive coupling of the lines connecting the active pixels to their digital cells. This effect varies with the pixel row position (see Figure 5). The time-walk originates from the fact that larger signals have shorter rise-time, and therefore cross the threshold earlier than smaller signals. This causes a ToA dispersion which is dependent on the signal height, and therefore on the ToT (see Figure 6). As both pixel row and ToT information are recorded for each hit, these effects can be measured and corrected.

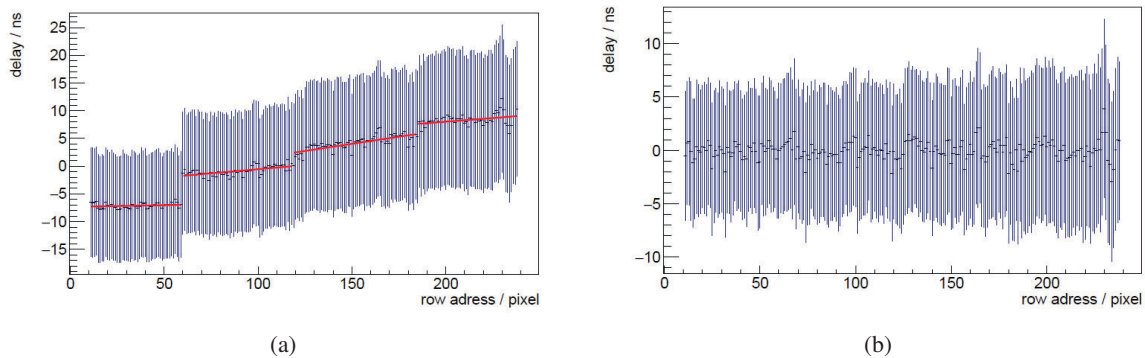


**Fig. 5.:** (a) Mean time difference between chip and scintillator for MuPix10 with a  $\text{Sr}^{90}$  source as a function of the hit row position. The linear dependency is extrapolated for four different regions. (b) Mean time difference between chip and scintillator for MuPix10 with a  $\text{Sr}^{90}$  source as a function of the hit row position, after correction. In both plots, the error bars are derived from the RMS of the time difference distribution [9].

Figure 7 shows that after these corrections the time resolution can be as low as 8.06(7) ns, well within the experimental requirement of 20 ns.

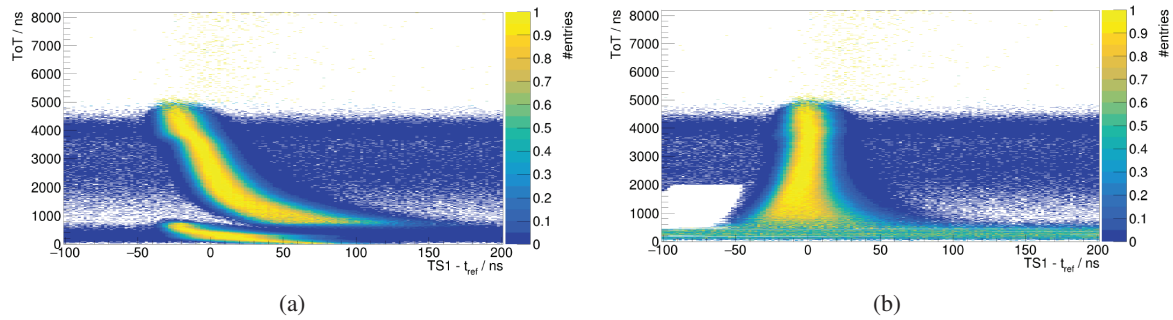


**Fig. 6.:** (a) Normalised 2D distribution of ToT and time difference between MuPix10 hit and scintillator for a  $\text{Sr}^{90}$  source. The region on the bottom left is due to cross-talk and can be filtered out [4]. (b) Normalised 2D distribution of ToT and time difference between MuPix10 hit and scintillator for a  $\text{Sr}^{90}$  source, after correction [9].

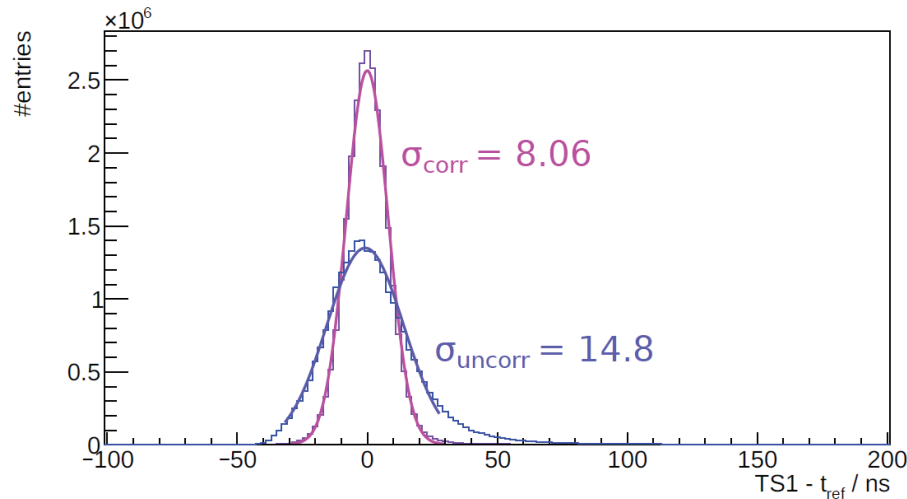


**Fig. 7.:** Distribution of time difference between MuPix10 hit and scintillator for a  $\text{Sr}^{90}$  source before (blue) and after (purple) row and time-walk corrections. The time resolution is calculated as the  $\sigma$  parameter obtained from the fit with a Gaussian function [9].

### 3.2 Thin Chips

The characterization of MuPix10 is completed by analyzing the performance of  $50\text{ }\mu\text{m}$  thin sensors, since this is the design thickness in the Mu3e experiment. The main effects to the performance in thinning the silicon bulk furthermore are observed in the leakage current and efficiency. The first effect is due to the fact that the full depletion can be reached earlier, the second is due to the reduction of the charge generation path and consequently of the average signal. The performance of the electronics, on the other hand, is not expected to change, since the circuitry is embedded on a thin layer on the top of the chip.

#### 3.2.1 Leakage Current

The first batch of  $50\text{ }\mu\text{m}$  thin MuPix10 chips with resistivity of  $370\text{ }\Omega\text{cm}$  is thinned via grinding without any further back-side processing. In this case, a sudden increase of leakage current is observed at about  $20\text{ V}$ , a much lower value than the breakdown voltage observed for  $100\text{ }\mu\text{m}$  thin

sensors. A more detailed thinning and measurement campaign has been conducted to study this behaviour at different thicknesses. The result is shown in Figure 8. As the thickness increases, the sudden increase in current is observed at higher voltage values. For each thickness, this value is compatible with the full depletion voltage considering a resistivity of  $370\ \Omega\text{ cm}$ . The current increase is explained by the depletion volume extending up to the grinded chip backside whose rough surface and microscopic cracks act as charge generation centers in the diodes electric field and thereby massively contribute to the current flow.

As a confirmation, the back-side of a  $100\ \mu\text{m}$  thin MuPix10 has been scanned using an AFM microscope (Figure 9). The effect of mechanical grinding can be clearly seen as the surface presents a high density of spikes which go as deep as  $200\ \text{nm}$ .

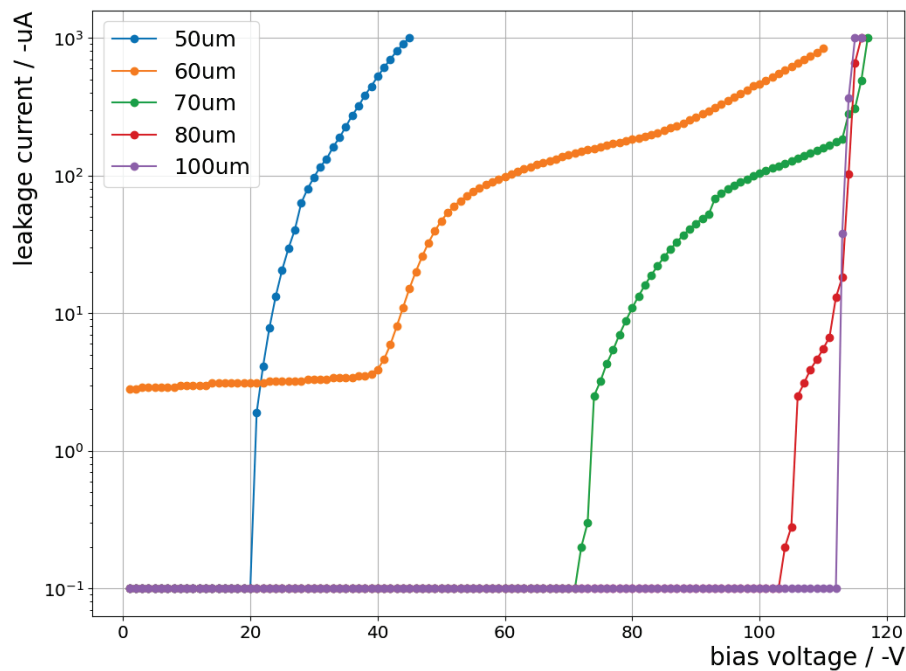


**Fig. 8.:** IV curve for MuPix10 samples at different thicknesses. Note: each curve corresponds to a different sensor which has been thinned with mechanical grinding [10].

This issue can be mitigated by treating the back-side of the chips [11]. In this case the method of plasma etching is chosen for the next production batches of MuPix11.

### 3.2.2 Efficiency

The efficiency of  $50\ \mu\text{m}$  thin MuPix10 sensors has been studied with a  $4\ \text{GeV}/c^2$  electron beam at the DESY test beam facility [12] and a telescope consisting of MuPix10 sensors. Since the device under test is not back-side processed with plasma etching, the voltage was kept at only  $20\ \text{V}$ . Nonetheless, as shown in Figure 10, the efficiency is observed to be higher than  $99\%$ . This value is better than the one showed for the  $100\ \mu\text{m}$  thin sensor at the same bias as a deep and extensive operation point optimization has been performed to maximize the signal amplitude.

Moreover, a tuning procedure has been developed to improve the efficiency. In contrast to the aforementioned procedure, this tuning strategy aims at reducing each pixel's threshold as low as

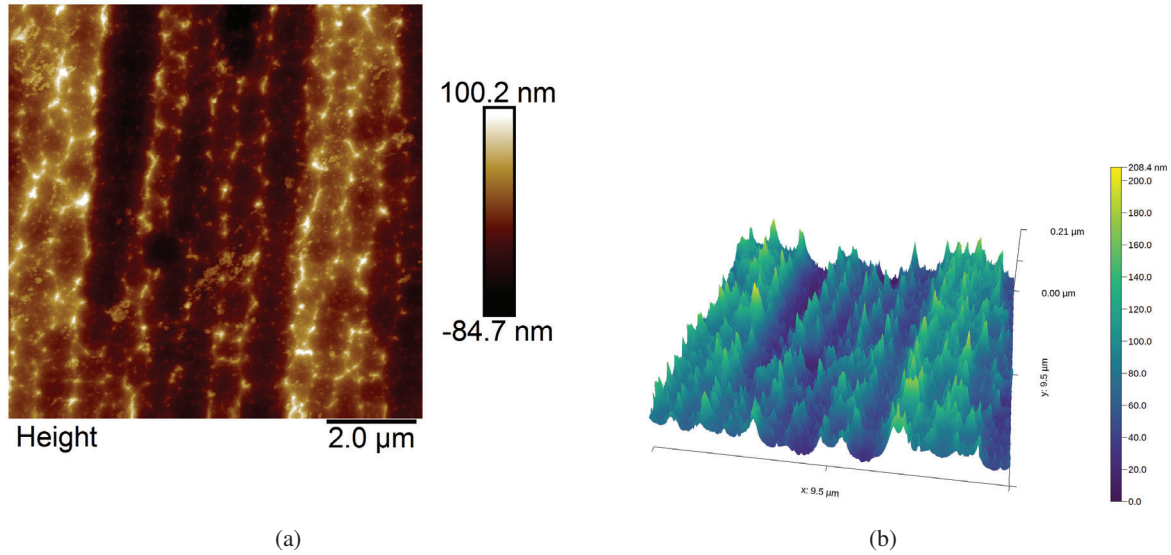


**Fig. 9.:** (a) AFM microscopy picture of the back-side of a 100  $\mu\text{m}$  thin MuPix10 sensor without back-side processing. (b) Height map of the surface obtained from the same sample [10].

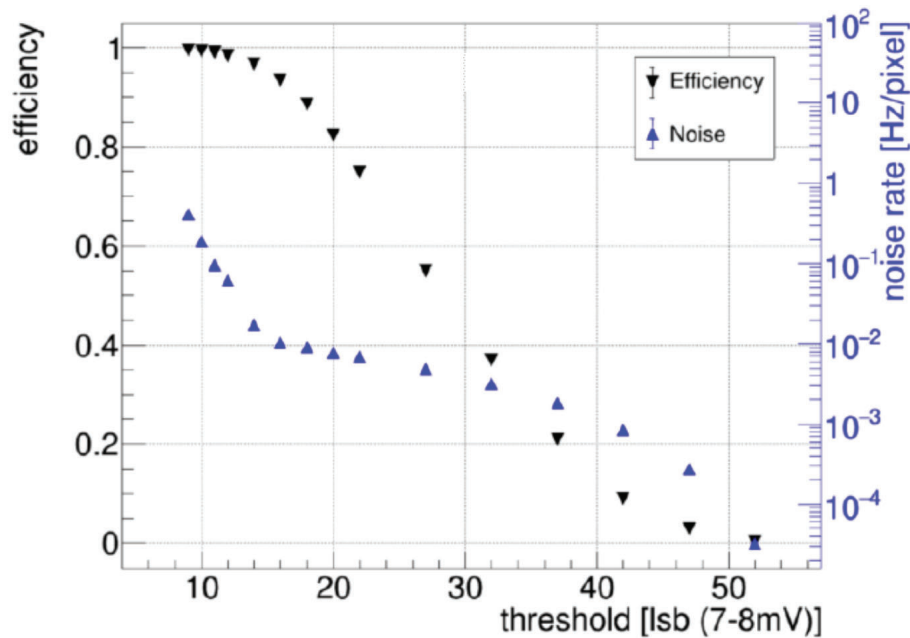


**Fig. 10.:** Efficiency and noise as a function of threshold for a 50  $\mu\text{m}$  thin MuPix10 sensor [10].

possible while keeping a maximum single pixel noise of 1 Hz (limited by DAQ). After this procedure is applied to a subset of pixels (about 15%), the effect on the efficiency is quite visible, with an improvement from 99.5% to 99.9% (see Figure 11).

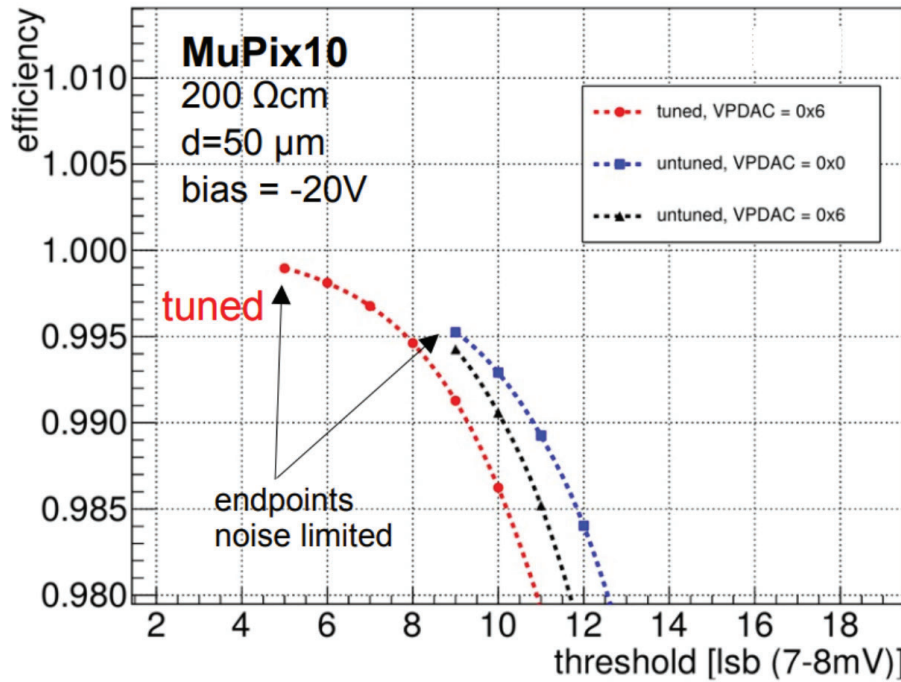


**Fig. 11.:** Efficiency as a function of threshold for a 50  $\mu\text{m}$  thin MuPix10 sensor at different configuration: without tuning (black and blue lines) and with tuning (red lines). The Note: VPDAC is the DAC responsible for the “strength” of the threshold corrections.

#### 4. Conclusion

The MuPix is an HV-MAPS specifically designed for the Mu3e experiment. From the first samples produced, the MuPix has been at the forefront of the HV-MAPS R&D. The latest samples, specifically MuPix10 and MuPix11, have gradually implemented the features required by the experiment.

A comprehensive R&D campaign has been performed on these samples, to prove that the experimental requirements can be met by the HV-CMOS technology. Several lab and test beam campaigns have been carried out, which verify that the efficiency and time resolution are within expectations. Some of the greatest challenges, in particular, are given by the strict experimental requirements for the thickness, which is limited to 50  $\mu\text{m}$ . The leakage current, for instance, increases significantly when the depletion region approaches the back-side, for which plasma etching is needed as back-side processing. Also, the thinner depletion region leads to less charge produced and therefore smaller signal. Nevertheless, the pixel threshold can be lowered enough for the efficiency to surpass 99% and yet keep the noise to a sustainable level.

All these results contributed to the qualification of the MuPix sensors for the Mu3e experiment, and the MuPix11 has been chosen as the baseline sensor of the Mu3e tracking system.

#### 5. Acknowledgements

H. Augustin, A. Meneses Gonzalez, D. M. Immig and A. Weber acknowledge support by the HighRR research training group [GRK 2058].

The measurements leading to these results have been performed at the Test Beam Facility at DESY Hamburg (Germany), a member of the Helmholtz Association (HGF).

Further, we would like to thank the Paul Scherrer Institute for providing high rate test beams under excellent conditions.

## References

- [1] K. Arndt et al., "Technical design of the phase I Mu3e experiment", NIM A, **volume 1014**, 165679, 2021.
- [2] I. Perić, "A novel monolithic pixelated particle detector implemented in high-voltage CMOS technology", Nucl.Instrum.Meth., **A582 876**, 2007.
- [3] H. Augustin et al., "Performance of the large scale HV-CMOS pixel sensor MuPix8", JINST **14 (10)** (2019) C10011.arXiv:1905.09309, doi:10.1088/1748-0221/14/10/C10011
- [4] H. Augustin et al., "MuPix10: First Results from the Final Design", JPS Conf.Proc. **34**, 010012, 2021.
- [5] LTU, LED Technologies of Ukraine – <https://www.ltu.ua/>
- [6] H. Augustin et al., "The Mu3e Data Acquisition", IEEE Transactions on Nuclear Science, **68**, 1833-1840, 2021
- [7] "The DESY II test beam facility", NIMA, **Volume 922**, 1 April 2019, Pages 265-28, (<https://doi.org/10.1016/j.nima.2018.11.133> )
- [8] J. Stricker, "Testing of a Method for the Sensor Thickness Determination and a Cluster Size Study for the MuPix10", Bachelor thesis, Heidelberg University, 2021
- [9] F. Frauen, "Time resolution studies of MuPix10", Bachelor thesis, Heidelberg University, 2021
- [10] D. Immig, "MuPix10: An Unexpected Journey", presentation for HighRR seminar, 30/03/2021, <https://indico.cern.ch/event/1134245/>
- [11] Hirono, Toko et al., "Depleted fully monolithic active CMOS pixel sensors (DMAPS) in high resistivity 150 nm technology for LHC", Nuclear Instruments and Methods in Physics Research Section A: Accelerators, Spectrometers, Detectors and Associated Equipment. **924. 10.1016/j.nima.2018.10.059**.
- [12] The DESY II test beam facility, ( <https://doi.org/10.1016/j.nima.2018.11.133> ) NIMA, **Volume 922**, 1 April 2019, Pages 265-28